Analyzing Aerosol Properties of Air Parcels Above Boone, NC, During the 2023 Summer Canadian Wildfire Season

Tess N. Mickey[a], Chris S. Thaxton[a], James P. Sherman[a], &Robert F. Swarthout[b]*

[a] *Department of Physics and Astronomy, Appalachian State University, Boone, NC*
[b] *A.R. Smith Department of Chemistry and Fermentation Sciences, Appalachian State University, Boone, NC*

https://doi.org/10.33697/ajur.2025.148

*Student: mickeytn@appstate.edu**
Mentors: thaxtoncs@appstate.edu, shermanjp@appstate.edu, swarthoutrf@appstate.edu

ABSTRACT
Air mass source regions and meteorological factors significantly influenced aerosol loading along air mass trajectories over Boone, North Carolina, between June 1, 2023, to August 31, 2023. This study examines the impact of northeast Canadian wildfires on aerosol loading, quantified by the particle light scattering coefficients at 550 nm measured at the NOAA Federated Aerosol Monitoring site at Appalachian State University (APP). Using NOAA's HYSPLIT trajectory model, hourly back trajectories originating at 500 meters above ground level at APP were analyzed over a 96-hour timespan and categorized into four aerosol loading classifications based on the aerosol light scattering coefficient at 550 nm measured at APP. All air parcel trajectories originating in eastern Canada were associated with the high and very high aerosol load classifications. Statistical analysis shows that wildfire-sourced parcels exhibit elevated temperatures and variability in solar flux. The findings establish a link between Canadian wildfire activity and increased aerosol loading in Boone, NC, emphasizing the relationships between source region, transport dynamics, and atmospheric conditions. These results provide a framework for further exploration of aerosol source regions and their broader environmental impacts.

KEYWORDS
Back-trajectory Analysis; HYSPLIT; Canadian Wildfires; Aerosols; Particle Light Scattering; Meteorology; Wildfire Impact; Air Mass Trajectories

INTRODUCTION

The Canadian fire season of 2023 was record-breaking, burning over 710,000 square miles.[1] Quebec, Northwest Territories, Alberta and British Columbia all faced unprecedented levels of tree cover loss due to wildfires in 2023 with Canadian wildfires making up 27% of the global tree cover loss for the year.[2] Significant fires included those in the Northwest Territories, where vast areas of forest and grasslands were affected. The fires were fueled by a combination of extreme heat, prolonged drought, and strong winds, which created ideal conditions for rapid fire spread and severe burning. Smoke from wildfires in Eastern Canada significantly impacted air quality across the Eastern United States. Numerous air quality alerts were issued through the summer of 2023, spanning regions from New England to the Midwest and the Southeast.

Fires in Eastern Quebec accounted for 29% of the total burned land in Canada between April and September 2023, with peak fire activity during June and July.[3] Smoke from these burns experienced transcontinental travel southeastward affecting populations downwind where the daily average $PM_{2.5}$ concentration peaked at 258.9 $\mu g/m^3$ in the northeastern United States. The World Health Organization defines $PM_{2.5}$ as particulate matter being 2.5 micrometers or less in diameter which can travel deep into the respiratory system; their air quality guideline recommends short-term exposure (24-hour) no more than 15 $\mu g/m^3$. [4] Increased exposure to $PM_{2.5}$ from wildfires affects respiratory, cardiovascular, and mental health, as well as birth outcomes. [5] In New York City, during the most intense smoke wave from June 6th to 8th, emergency department visits for asthma syndrome events increased from 181.5 per day in a reference period to 261 per day. [6] The ability to understand and predict the transport of wildfire smoke is increasingly important as the frequency of severe wildfire events has increased globally more than 2.2-fold in the last 20 years.[7]

Wildfires emit a complex mixture of gases and aerosols, primarily carbon dioxide, carbon monoxide, methane and short-lived organic aerosols and black carbon aerosols.[8] Black carbon aerosols absorb incoming solar radiation particularly well, making these emissions nearly as efficient as carbon dioxide at contributing to global warming.[9] Aerosols suspended in the atmosphere scatter incoming sunlight, reducing the amount of solar energy that reaches the surface- this is known as direct radiative forcing. Aerosol scattering also produces indirect effects, including cloud formation and alteration of meteorological processes. According to the

most recent Intergovernmental Panel on Climate Change Assessment Report (IPCC AR6, 2022)), aerosol-cloud interactions and aerosol direct radiative forcing due to scattering and absorption of sunlight by aerosols represent the largest sources of uncertainty in anthropogenic climate forcing.[10]

Located at the highest point on the Appalachian State University (APP) campus in Boone, NC (36.21°N, 81.69°W, 1080 m above sea level), the Appalachian Atmospheric Interdisciplinary Research facility (AppalAIR) is uniquely positioned to advance understanding of Southeastern U.S. (SE US) aerosols, precursor gases, and aerosol effects on regional air quality, cloud-aerosol processing, and the solar radiation budget. APP is home to the only co-located NOAA Federated Aerosol Network (NOAA FAN), NASA Aerosol Robotic Network (NASA AERONET), and NASA Micro-pulsed Lidar Network (MPLNET) sites in the U.S.. Lower tropospheric, column-averaged, and vertically-resolved aerosol optical and physical properties and concentrations are continuously measured at the site.[11–14] Refractory black carbon (BC) aerosol mass is estimated from aethalometer measurements of spectral aerosol light absorption. A meteorological station is also located on the aerosol sampling tower, located 34 m above ground level (AGL). The site is regularly exposed to air masses influenced by diverse potential aerosol sources: sulfate aerosols from power plant emissions to the west and northwest, anthropogenic organic aerosols (OA) and secondary OA (SOA) from major cities to the west, biogenic OA and SOA from the surrounding forests in the Appalachian Mountains, and BC aerosols from fossil fuel combustion and biomass burning.[16, 17]

Previous air mass transport and meteorology studies using AppalAIR data have suggested seasonal variation in aerosol sources. For example, Kelly *et al.* (2013) identified that synoptic weather patterns influenced the precipitation events in the southern Appalachian Mountain (SAM) region over a 16-month period in 2009 to 2010.[15] By combining these weather patterns with air mass back-trajectories, they determined statistical relationships between aerosol type and concentration during precipitation events measured at AppalAIR. Warm season trajectories were associated with greater aerosol loading by larger particles, consistent with oxidized, anthropogenically influenced sulfate and organic particles, whereas cool season trajectories were correlated with lower aerosol loading by particles that were thought to derive from regional biofuel burning (e.g. wood and coal stoves for residential heating).

In this study, air mass back trajectories were created hourly from June 1st to August 31st of 2023 using NOAA's HYSPLIT model. We classified each hourly trajectory using hourly-averaged aerosol light scattering coefficients measured at the NOAA FAN site at AppalAIR and further analyzed these trajectories through HYSPLIT. Our goal was to determine a relationship between origin areas of the most polluted air parcels that traveled over Boone, NC and the apportioned aerosol sourcing from Canadian wildfires. Meteorological variables from each trajectory group were statistically analyzed to uncover correlations between weather patterns and aerosol loading from these regions.

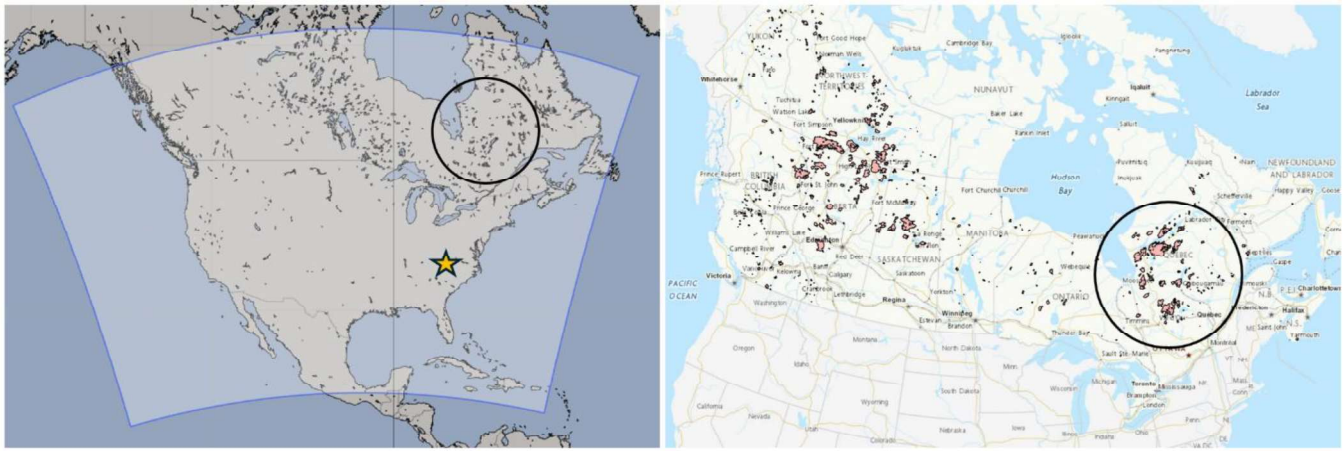

Figure 1. [LEFT] The NAM 12-km domain bounded by 152.9W, -49.4E, 12.1N, and 61.0S (from the National Centers for Environmental Information *https://www.ncei.noaa.gov/access/metadata/landing-page/bin/iso?id=gov.noaa.ncdc:C00630*). [18] The AppalAIR site is indicated by the gold star. [RIGHT] Burn area is highlighted in orange on the map during June 2023 (from the Fire Information for Resource Management System (FIRMS) *https://firms.modaps.eosdis.nasa.gov/*).[19] The general region of interest from Canadian wildfires is identified with the black circle.

METHODS AND PROCEDURES

NOAA's atmospheric transport and dispersion modeling system, Hybrid Single-Particle Lagrangian Integrated Trajectory (HYSPLIT), is widely used in simulations to describe the movement, distribution, and settling of pollutants in the atmosphere.[21] HYSPLIT has been used across diverse studies, including tracking and forecasting radioactive material, wildfire smoke, wind-blown dust, and other pollutants from natural and anthropogenic sources.[21, 22] HYSPLIT generates trajectories using the

integration method of Lagrangian modeling.[22–24] HYSPLIT back trajectories enable us to explore the source-receptor connection and the timeframes involved in long-range and local transport.[25]

HYSPLIT version 5.2 offers a variety of ways to further analyze meteorological data and back trajectories. Cluster analysis merges back trajectories into groups by minimizing the differences within an individual cluster and maximizing the differences between all clusters.[20, 27] These clusters become distinctive groups, which in recent years have been used to interpret atmospheric pollution.[26] In this study, we cluster HYSPLIT back trajectories by source region to isolate Canadian wildfire smoke and correlate the smoke with aerosol measurements made at AppalAIR for the Summer of 2023. We also employ HYSPLIT's trajectory frequency analysis which overlays a grid and displays the number of trajectories that intersect in each grid cell, normalized by the total number of trajectories.[27]

To generate back trajectories for clustering, we used the North American Mesoscale Forecast System (NAM) 12km datasets (found at *https://www.ncei.noaa.gov/metadata/geoportal/rest/metadata/item/gov.noaa.ncdc:C00630/html*) over the date range June 1, 2023, to August 31, 2023, as input to HYSPLIT.[18] Since the NAM domain is constrained to the Continental U.S. and Canada (CONUS), as shown in **Figure 1**, we limited the back trajectory time range to 96 hours; otherwise, too many back trajectories would terminate beyond the CONUS region and would be excluded from clustering and frequency analysis, especially for parcels at high altitudes subject to long-range synoptic transport. We ran HYSPLIT 96-hour back trajectories for every hour over the date range June 1, 2023, to August 31, 2023, to generate 2208 back trajectories that terminate at 500 m above ground level in Boone, NC (36.2N, 81.69W, 1080 m AGL). Note that this height is the height of the parcels at their "final" trajectory location – for example, some parcels at 500 m in Boone, NC, may have traveled well above the planetary boundary layer during transport. Even at the 96-hour back trajectory limit, roughly 7.6% of the back trajectories exceeded the NAM domain at the 500 m height and were discarded by HYSPLIT in later analysis.

Each 96-hour trajectory ending at Boone, NC, was classified into low, average, high, or very high aerosol loading bins based on hourly-averaged aerosol light scattering coefficient at 550 nm. Aerosol light scattering coefficient serves as a proxy for aerosol loading because it is directly proportional to both the aerosol number and mass concentrations, multiplied by the particle-scattering cross section and mass-scattering efficiency, respectively. Ambient air is sampled from a 34 m tower (well above the tree line) and gently heated to reduce the relative humidity (RH) of the air stream to less than 40% before entering the instruments, in accordance with standard NOAA aerosol sampling protocols.[11] Sampling at low RH decouples the confounding influences of RH and intrinsic aerosol properties on the measured scattering coefficients. The nephelometer measures light scattered in the angular range 7–170 degrees. Angular truncation effects and nephelometer light source idealities are corrected using the measured aerosol light scattering Angstrom exponent and the measured scattering coefficients are converted to their values at STP conditions (101.3 kPa, 0° Celsius) to facilitate comparisons with other sites.[29] The uncertainty in measured light scattering coefficient is approximately 10%.[28] The "low" aerosol loading classification is for hours where the measured scattering coefficient at 550 nm was less than 30 Mm^{-1}, where 1 $Mm^{-1} = 10^{-6}\ m^{-1}$. The "average" corresponds to scattering coefficients between 30 and 70 Mm^{-1}, "high" corresponds to 70 to 100 Mm^{-1}, and "very high" corresponds to a scattering coefficient greater than or equal to 100 Mm^{-1}. The classifications were determined based on 15 years of aerosol light scattering measurements at APP.[30] Trajectory clusters were generated, and frequency analysis performed at four different heights (500 m, 1500 m, 3500 m, and 5500 m) and four different aerosol load classifications (Low, Average, High, Very High) per height. In our meteorological analysis herein, we focus strictly on the 500 m heights since this corresponds to air parcels that reside within the planetary boundary layer from which the aerosol measurements were taken. We also used range-time images of normalized relative backscatter measured by the micro-pulsed lidar at APP to verify that the lower atmosphere below ~500–1000 m was well-mixed during most hours of the summer 2023 period under study, further justifying the usage of near-surface aerosol light scattering coefficients along with trajectories beginning at 500 m above the APP site.

In HYSPLIT, clustered trajectories are determined using an iterative method to minimize the total spatial variance (TSV). The TSV is a sum of the spatial variance of each cluster, where the spatial variance is the sum of the squared distances between the cluster-mean trajectory endpoint and the endpoints of that cluster's component trajectories.[23] **Figure 2** displays the percent change in TSV relative to the number of trajectory clusters for each aerosol load classification. The optimal number of clusters corresponds to the number of clusters prior to the rise in the TSV%.[27] In **Figure 2**, this criterion suggests retaining as many as eight clusters, particularly evident in the top-left and bottom-left panels for the low and high aerosol classifications, respectively. However, in all panels, the percentage change in TSV remains minimal for four clusters before rising sharply as the number of clusters decreases. Thus, we chose to limit our analysis to four clusters which is consistent with the objective percentage change criterion between 20% and 30% as recommended in the HYSPLIT documentation.[27]

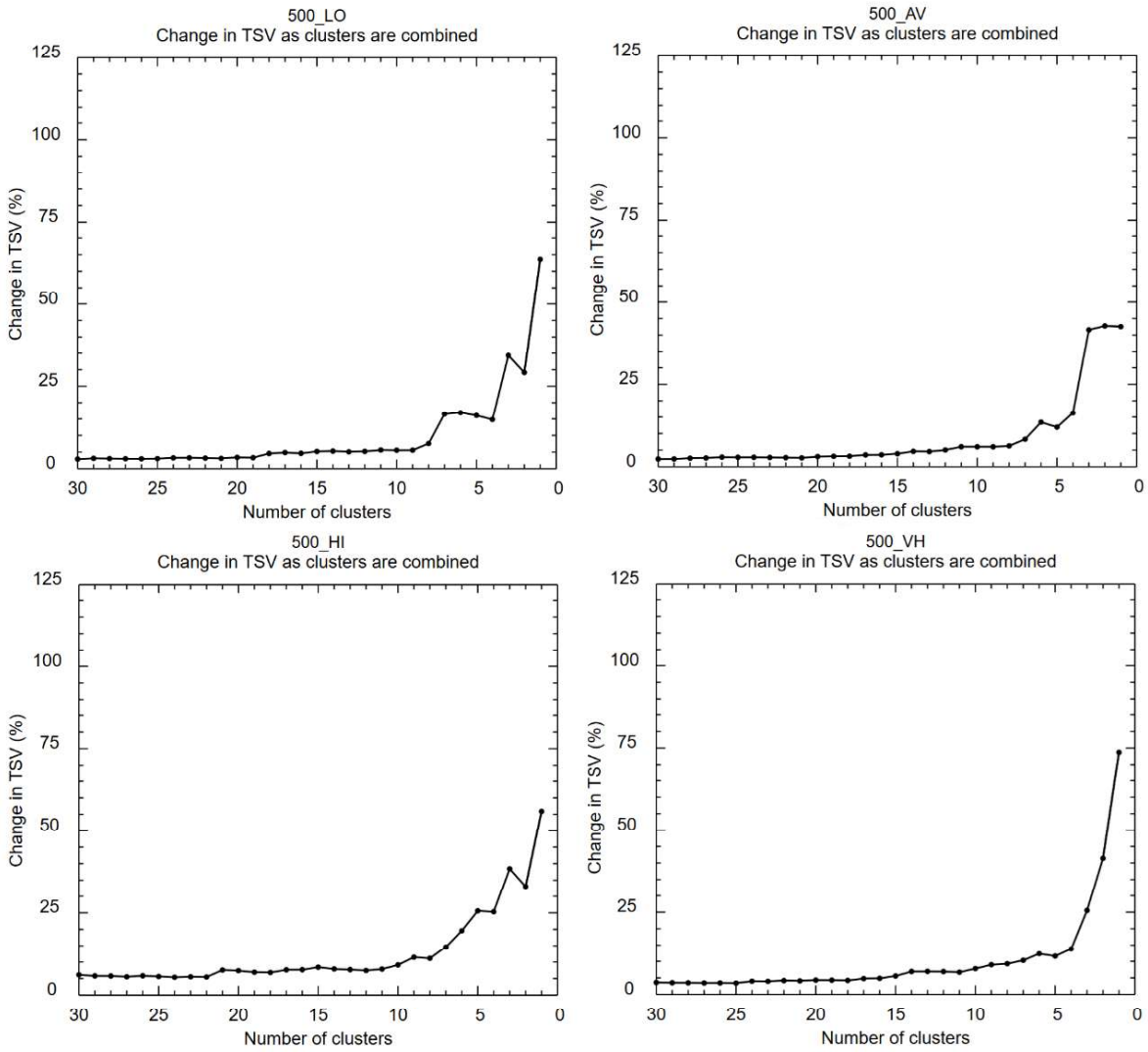

Figure 2. Percent change in TSV versus the number of clusters for each set of back trajectories at 500 m height for all aerosol load classifications. The low aerosol classification is shown in the top-left panel, the average in the top-right, the high in the bottom-left, and the very high in the bottom-right. The change in TSV informs the optimal number of clusters for our analysis. Four clusters is an appropriate choice as it marks the point where the percentage change in TSV has yet to sharply increase above 25% in all panels.

Each back-trajectory output file, *tdump*, contains meteorological variables for air parcels along the trajectory at every hour, including pressure [hPa], potential temperature [K], solar flux [$W \cdot m^{-2}$], mixing depth [m], relative humidity [%], air temperature [K], and precipitation rate [mm/hr]. For each *tdump* file, statistics such as the mean, median, maximum, and minimum were calculated for these variables. After clustering, a master database was created for each height (500 m, 1500 m, 3500 m, and 5500 m), containing the cluster number, aerosol load classification, and meteorological statistics for each aerosol observation hour. The master database enables analysis of the relationships between aerosol load and meteorology across various source regions, including those affected by the Canadian wildfires.

RESULTS AND DISCUSSION

The results of the back trajectories can be visualized in a full trajectory map. **Figure 3** shows the maps of every trajectory in each aerosol loading classification at the 500 m height. Of the 2040 valid back trajectories at the 500 m height, 744 were in the low aerosol loading classification, 891 in the average, 137 in the high, and 268 in the very high. The trajectory frequency analysis results complement the full back trajectory map by providing information on the local density and overall shape of trajectory paths, such as the curvature and divergence from the cluster mean for each category (see **Figure 4**). For the low aerosol load classification (**Figures 3a** and **4a**) and average aerosol load classification (**Figures 3b** and **4b**), the trajectories from the northeast U.S. and Eastern Canada originate east of the regions with wildfire activity and transport along the northeastern U.S.. For the high aerosol load classification category, **Figures 3c** and **4c**, the trajectories show inward spiraling from the Southwest and from the

middle region of Canada near the 100°W longitude line. For the very high aerosol load classification, **Figures 3d** and **4d**, many trajectories travel from Northeastern Canada inland, west of the Appalachian Mountain range. The high and very high share common trajectory structures that originate from or transport through the active wildfires in Canada.

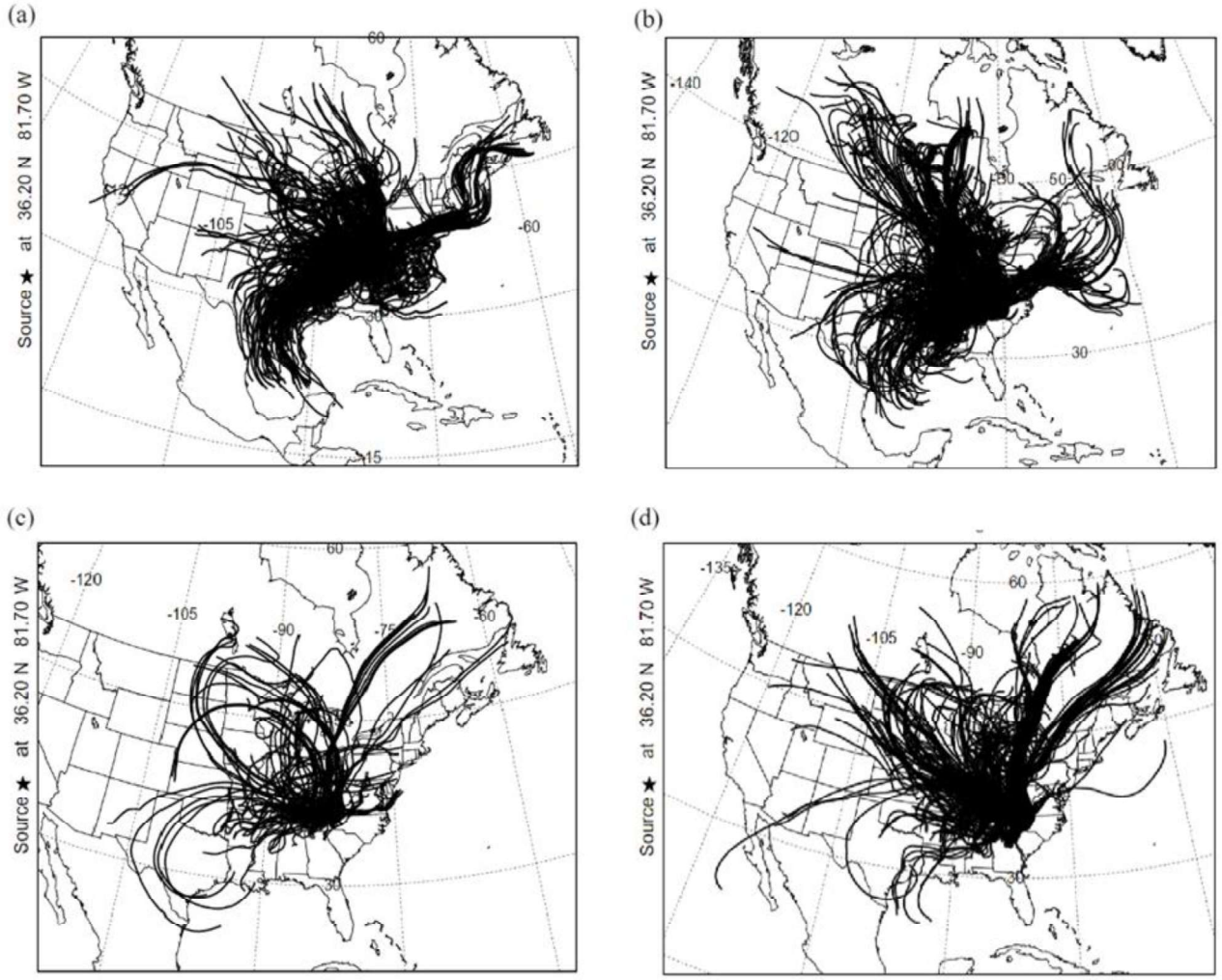

Figure 3. The HYSPLIT back trajectory map of each aerosol loading classification at 500 m. (a) low, (b) average, (c) high, (d) very high. Each line represents one 96-hour back trajectory with its starting point at 500 m above ground level in Boone, NC.

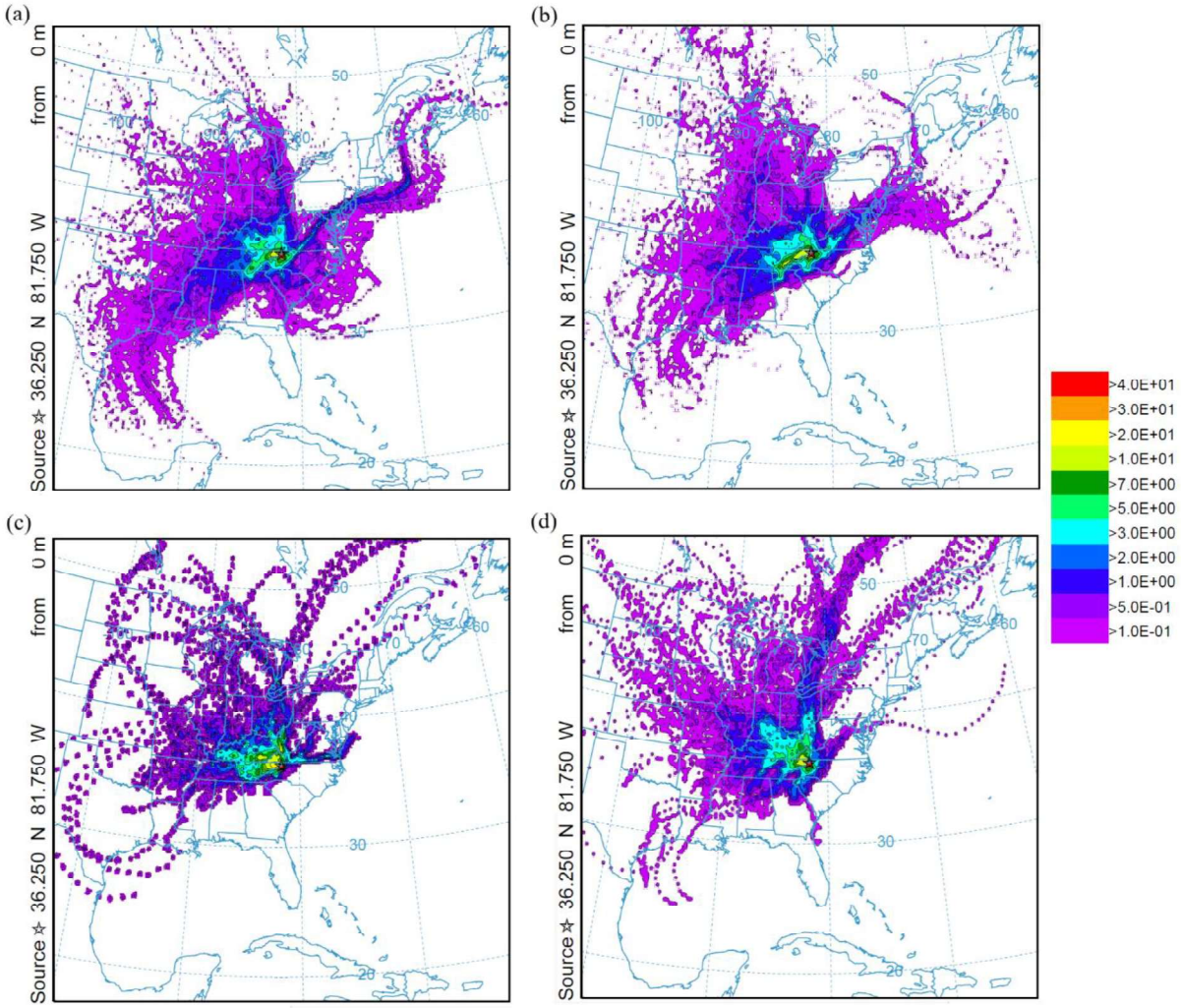

Figure 4. The results of trajectory frequency analysis at 500 m height based on aerosol classification (a) low, (b) average, (c) high, and (d) very high aerosol loading. The color-coded legend on the right indicates the number of trajectories intersecting each grid cell, normalized by the total number of trajectories for the corresponding aerosol classification.

Figure 5 shows the clustered trajectories for four clusters per aerosol load classification for the 500 m height. HYSPLIT automatically generates cluster numbers and colors for the trajectories that are not consistent between the aerosol classifications. To clarify the cluster results, we identified the clusters by source regions via regional identification acronyms (see **Table 1**). The trajectories come from five distinct regions: Eastern Maritime US (EMUS), North Central US (NCUS), South Central US (SCUS), Eastern Canada (ECAN), and the Ohio and Tennessee Valleys (OTVS) which represents the local region for the context of this study. **Table 1** also shows the number of trajectories per cluster. Trajectories unable to be clustered were discarded from the analysis by HYSPLIT, so the number of trajectories that were properly clustered is shown in the last row of **Table 1**.

Per **Figure 5**, the low and average aerosol classifications together account for 80% of all back trajectories and exhibit similar cluster trajectory paths, source regions and statistical distributions. Trajectories from the EMUS region contain no high or very high aerosol loads, while those from the SCUS region lack very high aerosol loads. In contrast, ECAN sourced clusters were classified into the high or very high aerosol load classifications throughout the study period. The local OTVS region sources more back trajectories than any other source region and contains the highest number of trajectories for all aerosol load classifications.

At the bottom of each panel in **Figure 5**, the parcel heights are plotted in meters above sea level (ASL) in which all back trajectories end in Boone, NC, at 500 m AGL, or 1470 meters ASL. The OTVS and EMUS air masses typically travel at altitudes below 1000 meters, corresponding to pressures around 898.8 hPa.[31] These lower-altitude air masses may carry aerosols or pollutants from regional emissions sources, such as vehicular or industrial emissions. In contrast, air masses originating from Canada in **Figure 5d** can reach altitudes as high as 3000 m, where the pressure drops to approximately 701.2 hPa. The higher

altitude at which these air masses travel suggests a different set of emission sources, potentially related to larger-scale agricultural activity and biomass burning. The differences in transport heights and aerosol loading between these air masses in **Figure 5** underscore the importance of considering both vertical and horizontal transport processes in the study of aerosol dynamics.

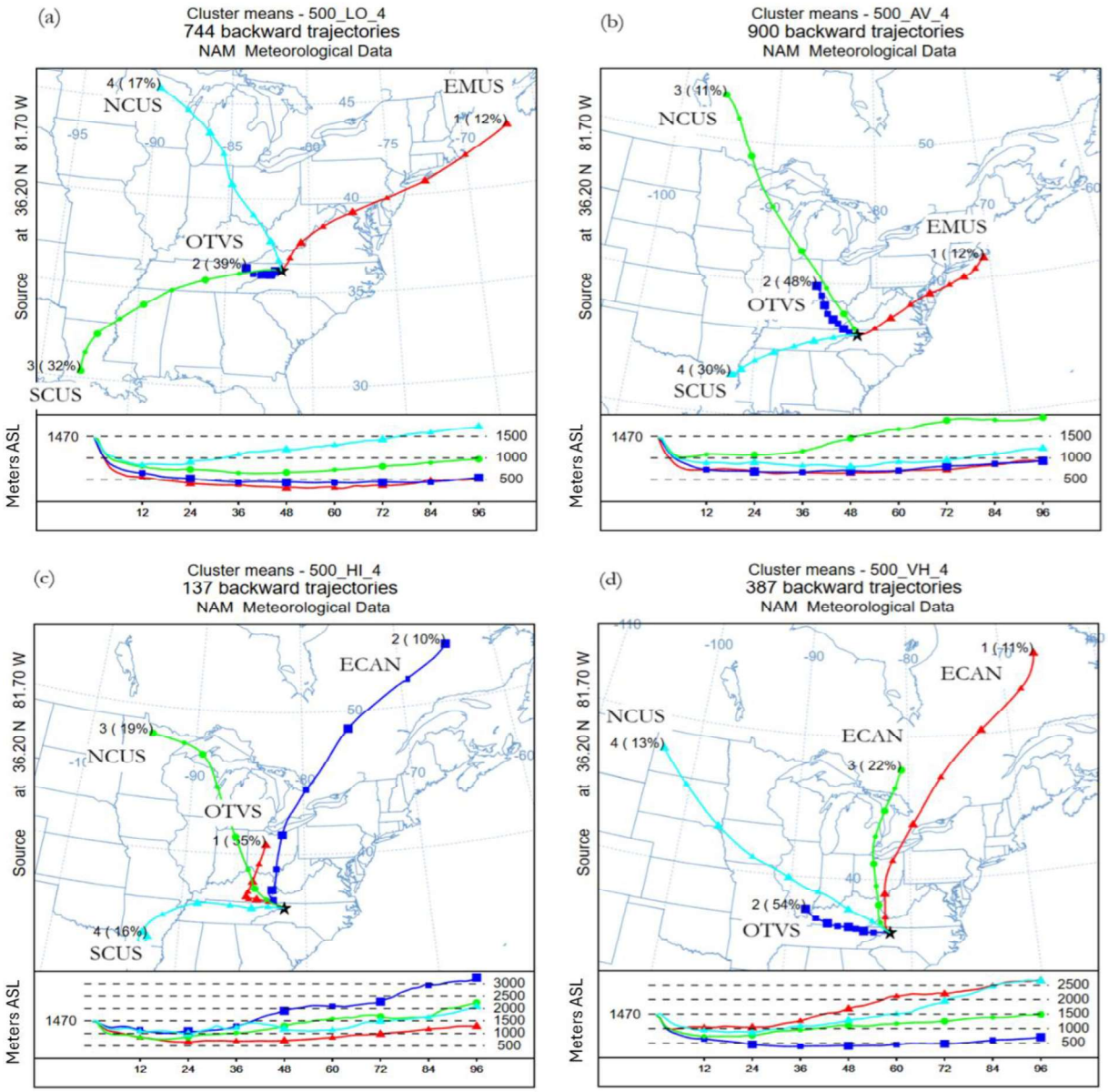

Figure 5. The results of HYSPLIT cluster analysis set to four clusters with meters ASL along the trajectory path shown below CONUS map for aerosol classification (a) low, (b) average, (c) high, and (d) very high. Each of the four cluster trajectories for low, average, high, and very high aerosol classifications are labelled with a source region ID that is detailed in **Table 1**. The total number of trajectories input for each classification is shown below the title of each panel, and the percentages next to the trajectory lines correspond to the proportion of total trajectories associated with each classification. Trajectories unable to be clustered were discarded from the analysis by HYSPLIT, so the number of trajectories that were properly clustered is shown in the last row of **Table 1**.

500 m Back-trajectories	Aerosol Load Classification							
	Low	**#**	**Average**	**#**	**High**	**#**	**Very High**	**#**
HYSPLIT Cluster – to – Source Region Identifier	C1 = EMUS C2 = OTVS C3 = SCUS C4 = NCUS	88 290 240 126	C1 = EMUS C2 = OTVS C3 = NCUS C4 = SCUS	104 429 85 273	C1 = OTVS C2 = ECAN C3 = NCUS C4 = SCUS	75 14 26 22	C1= ECAN C2 = OTVS C3 = ECAN C4 = NCUS	29 145 59 35
Number of Trajectories		744 (36%)		891 (44%)		137 (7%)		268 (13%)

Table 1. Clustered Source Region Acronyms. HYSPLIT Cluster – to – Source Region Identifier for each aerosol classification as shown in **Figure 5**. The source region identifiers are defined as: EMUS = Eastern Maritime US; NCUS = North Central US; SCUS = South Central US; OTVS = Ohio and Tennessee Valleys (local); ECAN = Eastern Canada. Analysis is performed for the 500 m final height back trajectories only. Also shown are the total number of trajectories per classification and cluster, and the total clusters and percentage of the total for each classification.

Figures 6–10 show statistical analysis of meteorological variables along the back trajectories' paths including parcel pressure [hPa], relative humidity [%] (RH), precipitation rate [mm/hr], air temperature [K], and solar flux [$W \cdot m^{-2}$]. Parcel pressures (**Figure 6**) are consistent with the clustered trajectory altitudes (**Figure 5**, bottom plots) for all source regions. The EMUS, SCUS, and OTVS exhibit the highest parcel pressures and lowest altitudes. The ECAN and NCUS exhibit the lowest pressures and highest altitudes. Early in the NCUS and ECAN trajectories, parcels are traveling above the mixing layer, subject to the higher wind speeds associated with synoptic scale transport and are spending less time in the mixing layer subject to localized influence. Outlying low pressures across all load classifications are most likely indicative of parcels being lifted to their final altitudes in Boone.

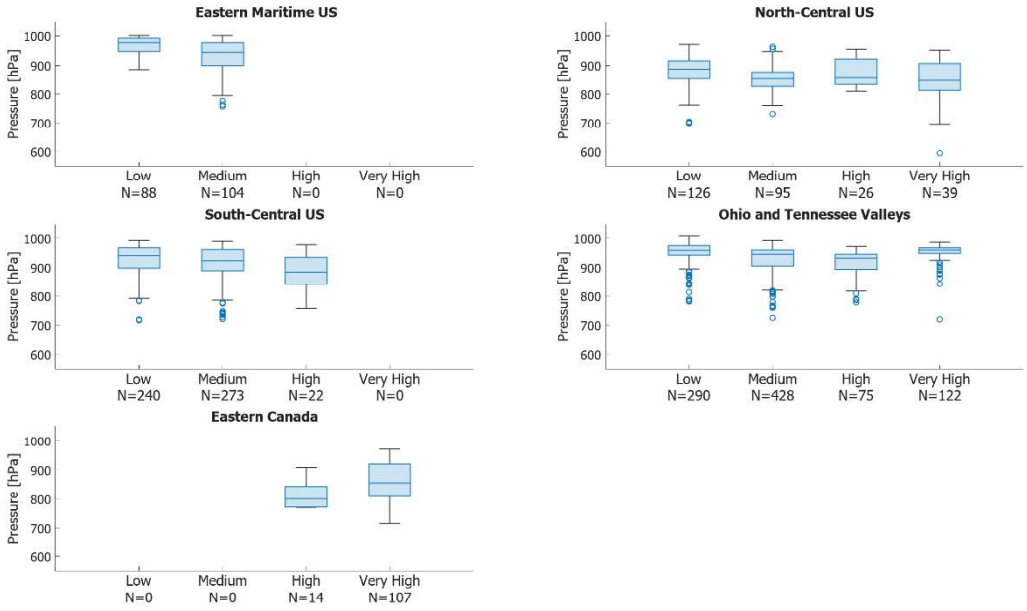

Figure 6. The results of statistical analysis of pressure [hPa] for each parcel along its back trajectory split into source region and aerosol classification boxplots.

Figure 7 is statistical analysis of solar flux values, in [$W \cdot m^{-2}$], for each clustered trajectory from each region. The median values for solar flux increase as aerosol load classification generally increases for every region. Solar flux promotes the formation of SOA within smoke, where VOCs are oxidized by sunlight and condense into new aerosol particles.[16] On the other hand, the presence of aerosols, once formed, tends to decrease solar flux due to absorption and scattering. In this study, we do not discern between the effects of diurnal aerosol processing and background wildfire smoke. At the local and regional scales (OTVS and SCUS), which are free of wildfire smoke, these results suggest that summertime aerosol loads at the local and regional scale positively correlate with solar flux, e.g. clear, sunny days lead to high aerosol loads whereas cloudy days suppress them. However, the aerosol load and solar flux for parcels from ECAN are negatively correlated, likely due to the presence of wildfire smoke and associated aerosols. The minimum value for solar flux in the very high aerosol classification is much lower for ECAN than the local and regional source regions. The large range for the quartiles and extrema in the boxplot for the ECAN very high aerosol load indicates that the very high aerosol load is only weakly dependent on the solar insolation at the source and along the trajectory paths to Boone, consistent with very high aerosol loads associated with the source wildfires.

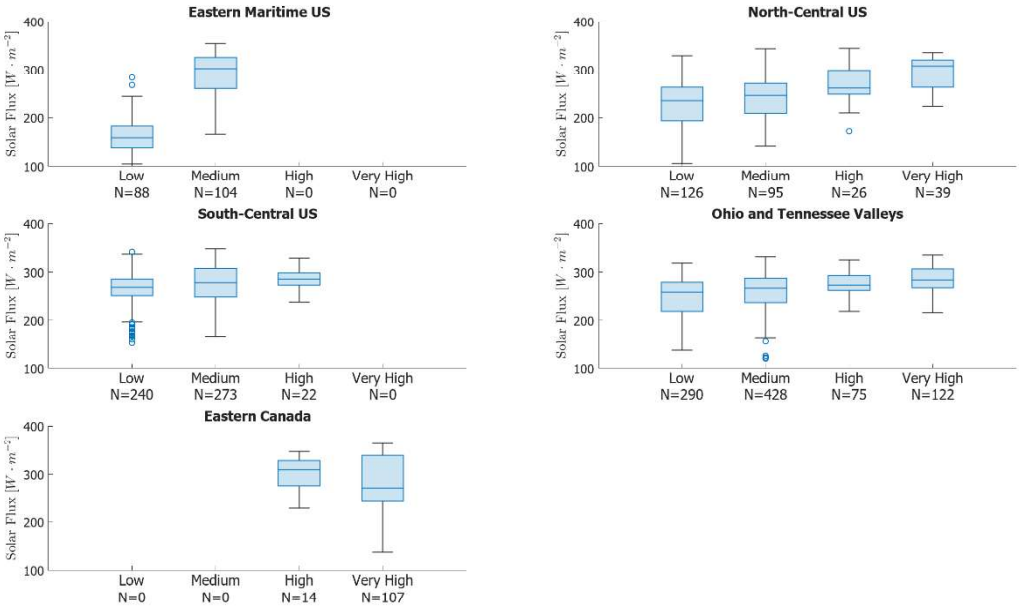

Figure 7. The results of statistical analysis of solar flux [W·m^{-2}] for each parcel along its back trajectory split into source region and aerosol classification boxplots.

Figure 8 shows boxplots for relative humidity (RH) by source region and aerosol load. For most regions, RH generally decreases as aerosol load increases except for the high and very high aerosol classifications of NCUS and ECAN. High RH generally enhances the liquid-phase reactions of trace gases and increases aerosol formation, suggesting that this analysis should show the opposite trend – that aerosol loads should increase with RH levels regardless of source region. However, competing processes such as cloud wet scavenging make it difficult to correlate RH levels with aerosol loads based on the data and analysis performed in this study with confidence.

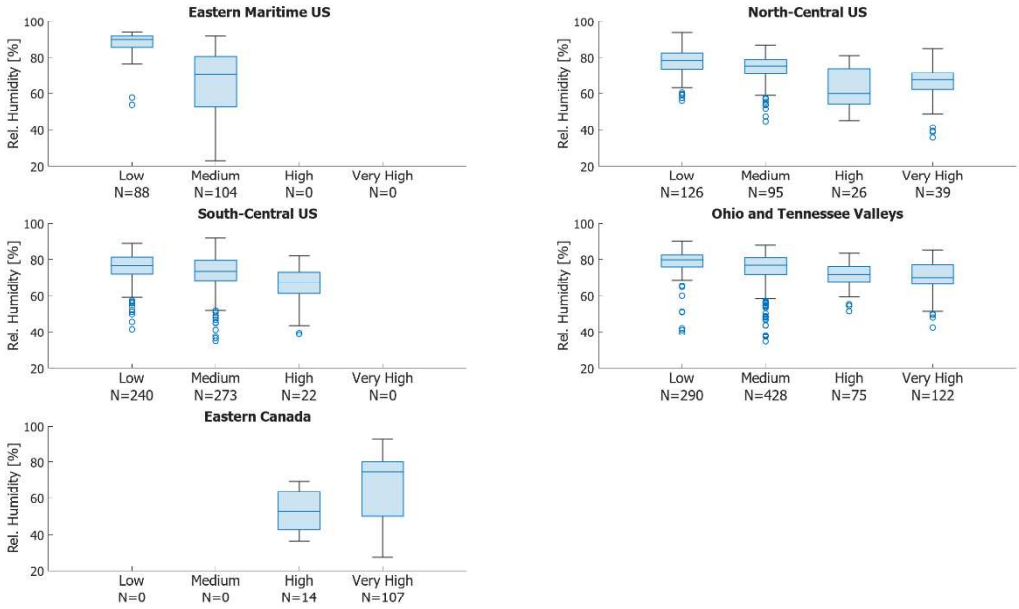

Figure 8. The results of statistical analysis of relative humidity [%] for each parcel along its back trajectory split into source region and aerosol classification boxplots.

Figures 9 and **10** show the precipitation rate [mm/hr] and air temperature [K] along the trajectory paths, respectively. As expected, aerosol loads drop with higher precipitation rate due to aerosol washout. Also as expected, air temperatures were lowest for the parcels out of ECAN, NCUS and EMUS, and highest for the SCUS and OTVS source regions. Generally, for each source region, air temperatures were roughly constant across all aerosol classifications. The exception is the unusually high air temperature for the very high out of ECAN which may correspond to the presence of sensible heat associated with aerosols released from biomass burning.

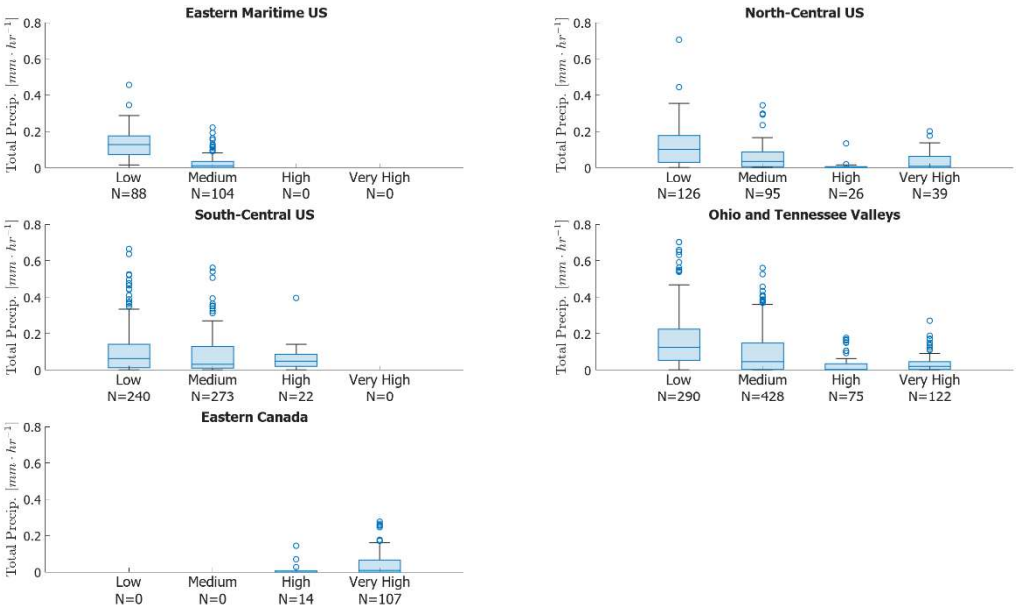

Figure 9. The results of statistical analysis of precipitation rate [mm/hr] for each parcel along its back trajectory by source region and aerosol classification.

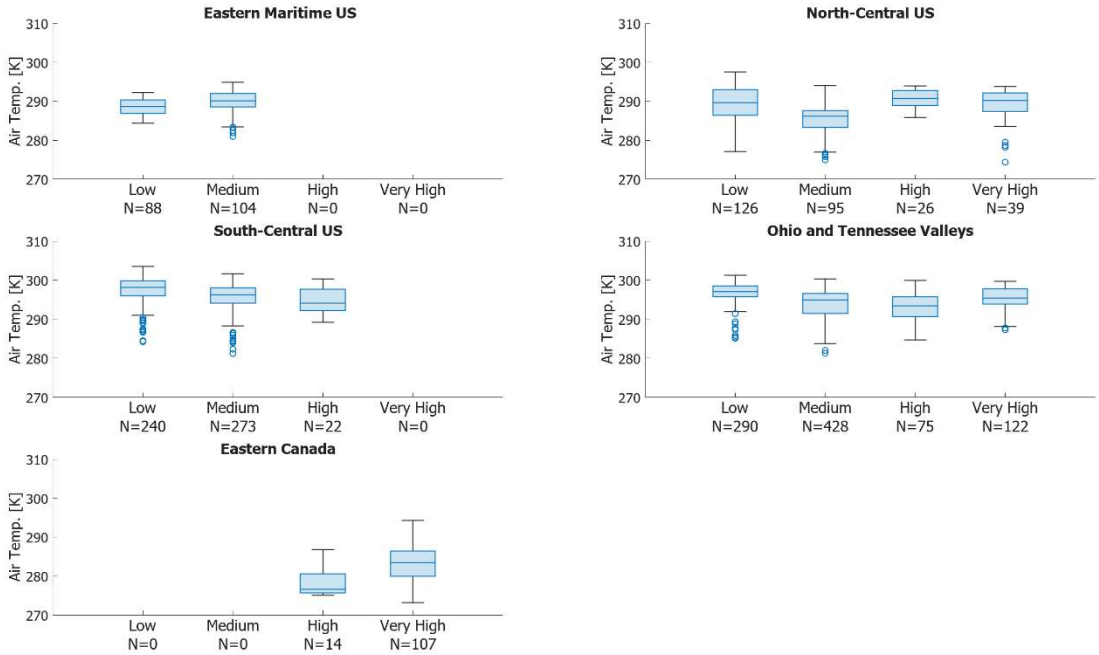

Figure 10. The results of statistical analysis of air temperature [K] for each parcel along its back trajectory split into source region and aerosol classification boxplots.

CONCLUSIONS

In this study, we sought to correlate the smoke transported from the eastern Canadian wildfires in the summer of 2023 with mid-visible aerosol light scattering measurements made at the NOAA FAN site in Boone, NC., over the same period. To simplify the analysis, we broke the aerosol light scattering measurements into aerosol loading classifications – low, medium, high, and very high – based on historical measurements made at the AppalAIR site on the Appalachian State University campus. We ran NOAA's HYSPLIT model at high temporal resolution for the summer months in 2023 and clustered the resulting back trajectories into five primary source regions, one of which is the Eastern Canada (ECAN) region from which the active wildfires emitted smoke throughout the summer season. HYSPLIT also provides meteorological information, allowing for the extraction of statistical meteorological characteristics for the parcels from each source region. The incorporation of aerosol load classification levels with HYSPLIT cluster analysis provides a comprehensive view of relationships between aerosol loading and source region as well as the meteorological conditions through which the parcels travelled.

HYSPLIT trajectory frequency and cluster analysis show distinct differences in the aerosol load classifications for each source region. Notably, the ECAN region contributes only to the high and very high aerosol loads consistent with Canadian wildfire activity during the summer of 2023. The meteorological analyses further relate to the influences of environmental factors along trajectory paths. Parcel pressure and altitude results indicate that trajectories from ECAN and NCUS travel at higher altitudes subject to synoptic scale transport. Increasing solar flux for the higher aerosol loading classifications suggest increased secondary organic aerosol formation with higher aerosol loads, though ECAN exhibits variability that aligns with wildfire contributions independent of solar insolation. Additionally, precipitation rates along each parcel trajectory follow the expected trend as precipitation effectively reduces aerosol loads, while higher air temperatures in ECAN trajectories within the very high aerosol load may reflect heat contributions from biomass burning events. Together, these findings connect source region, transport dynamics, and meteorological conditions to aerosol characteristics over Boone, NC. The contribution of Canadian wildfire emissions to high and very high aerosol classification loads underscores the role of regional wildfire activity in influencing aerosol transport and local atmospheric conditions. This analysis couples measurements of aerosol optical properties from a background SE US site with back-trajectory analysis to effectively identify aerosol source regions. Further research investigating other aerosol properties in cluster-mean trajectories would provide valuable insight into apportioned aerosol sourcing beyond the regions identified in this study. In addition, this study supports the need for synoptic and diurnal scale analysis to fully decouple traditional aerosol processing from the influences of long transport wildfire smoke.

REFERENCES

1. NASA. (2023) Tracking Canada's Extreme 2023 Fire Season. NASA Earth Observatory. *https://earthobservatory.nasa.gov/images/151985/tracking-canadas-extreme-2023-fire-seSon*
2. MacCarthy, J., Tyukavina, A., Weisse, M., Harris, N. (2024) Canada's Record-breaking 2023 Wildfires Made International Headlines. Here's What They Mean for Climate Change. World Resources Institute. *https://www.wri.org/insights/canada-wildfire-emissions*
3. Chen, Han; Zhang, Weihang; Sheng, Lifang. (2025) Canadian record-breaking wildfires in 2023 and their impact on US air quality. *Atmospheric Environment* 342:120941.
4. World Health Organization (WHO). (2021) WHO global air quality guidelines: particulate matter (PM2.5 and PM10), ozone, nitrogen dioxide, sulfur dioxide and carbon monoxide. WHO. 100–130.
5. Reid, C.E., Brauer, M., Johnston F.H., Jerrett M., Balmes J.R., Elliott C.T. (2016) Critical Review of Health Impacts of Wildfire Smoke Exposure. *Environ Health Perspectives,* 124(9), 1334–1343. *https://doi.org/10.1289/ehp.1409277*
6. Chen, K., Ma, Y., Bell, M. L., & Yang, W. (2023). Canadian Wildfire Smoke and Asthma Syndrome Emergency Department Visits in New York City. *JAMA*, *330*(14), 1385–1387. *https://doi.org/10.1001/jama.2023.18768*
7. Cunningham, C.X., Williamson, G.J., Bowman D.M.J.S. (2024) Increasing frequency and intensity of the most extreme wildfires on Earth. *Nat Ecol Evol* 8, 1420–1425. *https://doi.org/10.1038/s41559-024-02452-2*
8. Urbanski, Shawn. (2014) Wildland fire emissions, carbon, and climate: Emission factors. Forest Ecology and Management. 317: 51–60.
9. Ramanathan, V., Carmichael, G. (2008) Global and regional climate changes due to black carbon. *Nature Geosci* 1, 221–227 *https://doi.org/10.1038/ngeo156*
10. IPCC. (2022) *Climate Change 2022: Impacts, Adaptation, and Vulnerability*. Contribution of Working Group II to the Sixth Assessment Report of the Intergovernmental Panel on Climate Change [H.-O. Pörtner, D.C. Roberts, M. Tignor, E.S. Poloczanska, K. Mintenbeck, A. Alegría, M. Craig, S. Langsdorf, S. Löschke, V. Möller, A. Okem, B. Rama (eds.)]. Cambridge University Press. Cambridge University Press, Cambridge, UK and New York, NY, USA, 3056 pp., *https://doi.org/10.1017/9781009325844*
11. Andrews, E., Sheridan, P., Ogren, J.A., Hageman, D., Jefferson, A., Wendell, J., Alastuey, A., Alados-Arboledas, L., Bergin, M., Ealo, M., Hallar, A.G., Hoffer, A., Kalapov, I., Keywood, M., Kim, J.,

Kim, S.-W., Kolonjari, F., Labuschagne, C., Lin, N.-H., Macdonald, A., Mayol-Bracero, O.L., McCubbin, I.B., Pandolfi, M., Reisen, F., Sharma, S., Sherman, J. P., Sorribas, M., Sun, J. (2019) Overview of the NOAA/ESRL Federated Aerosol Network, *Bull. Amer. Meteor. Soc*., 100, 123–135. *https://doi.org/10.1175/BAMS-D-17-0175.1*

12. Holben, B.N., Eck, T.F., Slutsker, I., Tanre, D., Buis, J.P., Setzer, A., Vermote, E., Reagan, J.A., Kaufman, Y.J., Nakajima, T., Lavenu, F., Janowiak, I., Smirnov, A. (1988) AERONET—A federated instrument network and data archive for aerosol characterization, *Remote Sens. Environ*., 66, 1–16.
13. Welton, E. J. (1998) Ground-based lidar measurements of aerosols during ACE-2: Instrument description, results, and comparisons with other ground-based and airborne measurements, Tellus, Ser. B, 52, 635–650, 2000.0
14. Sherman, J.P. and A. McComiskey. (2018) Measurement-Based Climatology Of Aerosol Direct Radiative Effect, Its Sensitivities, And Uncertainties From A Background Southeast US Site, *Atmos. Chem. Phys*., 18, 4131–4152, 2018 *https://doi.org/10.5194/acp-18-4131-2018*
15. Kelly, G.M., Taubman, B.F., Perry, L.B., Sherman, J.P., Soule, P.T., Sheridan, P.J. (2013) Relationships between Aerosols and Precipitation in the Southern Appalachian Mountains. *Int. J. Climatol.* 33: 3016–3028.
16. Ortega, A. M., Day, D. A., Cubison, M. J., Brune, W. H., Bon, D., de Gouw, J. A., and Jimenez, J. L. (2013): Secondary organic aerosol formation and primary organic aerosol oxidation from biomass-burning smoke in a flow reactor during FLAME-3, *Atmos. Chem. Phys.,* 13, 11551–11571, *https://doi.org/10.5194/acp-13-11551-2013*
17. Link, M.F., Zhou, Y., Taubman, B.F., Sherman, J.P., Morrow, H., Krintz, I., Robertson, L., Cook, R., Stocks, J., West, M., Sive, B.C., (2015) A characterization of volatile organic compounds and secondary organic aerosol at a mountain site in the southeastern United States. *J. Atmos. Chem*., 72, 81104, *https://doi.org/10.1007/s10874-015-9305-5*
18. North American Mesoscale Forecast System (NAM) 12 km. Meso-ETA. National Centers for Environmental Information. NOAA. *https://www.ncei.noaa.gov/access/metadata/landing-page/bin/iso?id=gov.noaa.ncdc:C00630* (Accessed April 2024)
19. Fire Information for Resource Management System (FIRMS). NASA. *https://firms.modaps.eosdis.nasa.gov/* (Accessed April 2025)
20. Tao, W.K., Chen, J.P., Li, Z., Wang, C., Zhang, C. (2012) Impact of Aerosols on Convective Clouds and Precipitation. *Rev of Geophy*. Vol 50, Issue 2. *https://doi.org/10.1029/2011RG000369*
21. Stein, A.F., Draxler, R.R, Rolph, G.D., Stunder, B.J.B., Cohen, M.D., and Ngan, F. (2015) NOAA's HYSPLIT atmospheric transport and dispersion modeling system, *Bull. Amer. Meteor. Soc*., 96, 2059–2077, *http://dx.doi.org/10.1175/BAMS-D-14-00110.1*
22. Draxler, R.R., (1999) HYSPLIT4 user's guide. NOAA Tech. Memo. ERL ARL-230, NOAA Air Resources Laboratory, Silver Spring, MD.
23. Draxler, R.R., Hess, G.D. (1998) An overview of the HYSPLIT_4 modeling system of trajectories, dispersion, and deposition. *Aust. Meteor. Mag.,* 47, 295–308.
24. Draxler, R.R., Hess, G.D. (1997) Description of the HYSPLIT_4 modeling system. NOAA Tech. Memo. ERL ARL-224, NOAA Air Resources Laboratory, Silver Spring, MD, Pp. 24
25. Fleming, Z. L., P. S. Monks, Manning, A.J. (2012) Review: Untangling the influence of air-mass history in interpreting observed atmospheric composition. *Atmos. Res*., 104–105, 1–39, *https://doi.org/10.1016/j.atmosres.2011.09.009*
26. Abdalmogith, S.S., Harrison, R.M. (2005) The use of trajectory cluster analysis to examine the long-range transport of secondary inorganic aerosol in the UK. *Atmos Env*. Vol 39, Issue 35. Pp 6686–6695.
27. Draxler, R.R., Stunder, B., Rolph, G., Stein, A. Taylor, A., Zinn, S., Loughner, C., Crawford, A., (2022) HYSPLIT User's Guide. Run Cluster Analysis. NOAA Air Resources Laboratory, Silver Springs, MD. *https://www.arl.noaa.gov/documents/reports/hysplit_user_guide.pdf*
28. Sherman, J. P., P. J. Sheridan, J. A. Ogren, E. Andrews, D. Hageman, L. Schmeisser, A. Jefferson, and S. Sharma. (2015) A multi-year study of lower tropospheric aerosol variability and systematic relationships from four North American regions, *Atmos. Chem. Phys*., 15(21), 12487–12517, *https://doi.org/10.5194/acp-15-12487-2015*
29. Anderson, T. L., and J. A. Ogren. (1998) Determining aerosol radiative properties using the TSI 3563 integrating nephelometer. *Aerosol Sci. Technol.*, *29*, 57–69, *https://doi.org/10.1080/02786829808965551*
30. Swarthout, R., Linker, S., Davis, P., Hamrick, R., Huffenus, E., Sherman, J., Barber, E., Schonhoff, A., Ingram, E., Tischer, C., Thaxton, C., & Mickey, T. (2024). Aerosol chemical composition and optical properties observed at the Southeastern U.S. AppalAIR observatory. In *AGU Fall Meeting Abstracts* (pp. A31F-178).
31. NOAA, NASA, United States Air Force. (1976). U.S. Standard Atmosphere. Table 1 Geometric Altitude, Metric Units. Page 52–54. NOAA-S/T-76-1562

ABOUT STUDENT AUTHOR

Tess Mickey is currently attending Appalachian State University. She plans to graduate in the spring of 2025 with a bachelor's degree in applied physics with a minor in mathematics.

PRESS SUMMARY

This study investigates how smoke and aerosols from northeast Canadian wildfires during the summer of 2023 traveled to Boone, North Carolina, and influenced local air conditions. High and very high aerosol pollution levels were linked to air masses originating from wildfire-affected areas in Canada. Meteorological variables such as temperature, altitude, and sunlight interaction along air-parcel paths were tied to variations in aerosol levels. These findings emphasize the importance of understanding wildfire-driven air pollution and its long-range effects.